JOURNAL OF THERMOPHYSICS AND HEAT TRANSFER
Vol. 7, No. 1, Jan.–March 1993

Thermal Modeling of the Continuous Casting Process

B. H. Kang*
Korea Institute of Science and Technology, Seoul, Republic of Korea
and
Y. Jaluria†
Rutgers University, New Brunswick, New Jersey 08903

The transport processes in the mold and in the cooling zone for continuous casting have been simulated. This problem is of particular interest in several manufacturing technologies, such as metal casting, fiber glass drawing, plasting extrusion, and Czochralski crystal growing. A few one-dimensional, three-zone models have been developed and analytical solutions obtained. The location and shape of the liquid-solid interface and the temperature fields in the liquid and solid have been investigated. A two-zone model for one-dimensional problems has been also introduced to solve the problem, employing the finite-difference method. The enthalpy method with an assumed heat transfer coefficient at the surface of the material, has been employed to solve two-dimensional problems, considering the axial diffusion term and thermal buoyancy effects in the liquid. The full, elliptic equations are solved employing finite-difference techniques. The temperature and flowfields in the liquid zone and the mass fraction of the liquid are computed as solidification proceeds. The results obtained indicate good agreement with analytical solutions given in the literature for small Peclet number. The interface shape and the resulting temperature fields are found to be strongly dependent upon the cooling rate in the mold and the withdrawal speed of the solidified material. Axial diffusion is found to be important and the buoyancy effects to be small over the parametric ranges considered, which apply for several relevant processes in practice.

Nomenclature

A = cross-sectional area of cast material
Bi = Biot number, defined in Eq. (5)
C = specific heat of solid or fluid at constant pressure
d = half-thickness or radius of cast material
f_l = mass fraction of liquid
Gr = Grashof number, defined in Eq. (31)
g = magnitude of gravitational acceleration
H = enthalpy
H^0 = enthalpy evaluated at zero T
h = convective heat transfer coefficient
k = thermal conductivity
k_f = thermal conductivity ratio, k/k_s
L = latent heat of fusion
ℓ = mold length
ℓ_f = distance from inlet liquid level to the liquid-solid interface
ℓ_1 = distance from inlet liquid level to the inlet of the mold
ℓ_2 = distance from inlet liquid level to the end of the mold
m = mass fraction of solid in the mold
P = perimeter of cast material
Pe = Peclet number, defined in Eq. (5)
Pr = Prandtl number of the fluid, ν/α
p = local pressure
Re = Reynolds number, defined in Eq. (32)
Ste = Stefan number, defined in Eq. (5)
T = local temperature
T_m = melting or solidification temperature
t = physical time
U = dimensionless velocity component in x direction, u/U_s
U_s = withdrawal speed of the solid material
u = local velocity in x direction
V = dimensionless velocity component in y direction, v/U_s
v = velocity component in y direction
$\vec{V}$ = dimensionless velocity vector, $\vec{v}/U_s$
$\vec{v}$ = velocity vector
X = dimensionless x coordinate, x/d
x = coordinate distance in direction of material motion
Y = dimensionless y coordinate, y/d
y = coordinate distance normal to direction of material motion
α = thermal diffusivity, $k/\rho C$
β = coefficient of thermal expansion of the fluid
δ = solid thickness in the mold
θ = dimensionless local temperature, $(T - T_\infty)/(T_m - T_\infty)$
ν = kinematic viscosity of fluid in the interface zone
ν_r = ratio of the kinematic viscosity ν/ν_l for liquid-solid interface zone
ρ = density
τ = dimensionless time, tU_s/d
Ψ = dimensionless stream function, $\psi/U_s d$
ψ = stream function
Ω = dimensionless vorticity, $\omega d/U_s$
ω = vorticity
$\tilde{\omega}$ = relaxation factor

Subscripts
k = phase designation
l = liquid
m = melting point
s = solid
0 = inlet of liquid
1 = liquid zone
2 = mold zone
3 = secondary cooling zone
∞ = ambient

Superscript
$*$ = dimensionless quantity

Received June 10, 1991; revision received March 11, 1992; accepted for publication March 13, 1992.

*Air-Conditioning and Environmental Control Laboratory.
†Department of Mechanical and Aerospace Engineering.

Introduction

CONTINUOUS casting is a very important manufacturing process, particularly for metals, since it offers several advantages. The microstructure of the metals processed by continuous casting is dendritic (as in casting in an enclosed region), but is more dense and uniform because the whole length receives the same treatment in the mold. In addition, the continuous casting process is essentially automatic and the unit labor cost is low. Dies or molds are made of copper or graphite and are simple and inexpensive. The basic process involves the flow of the molten material in a mold, which is often water cooled, followed by a high cooling rate downstream. This results in the solidification of the liquid across a phase interface and the solidified ingot is withdrawn at a uniform velocity U_s. The process under consideration is also similar to several other manufacturing techniques, such as fiber glass drawing, plastic extrusion, and Czochralski crystal growing.[1-3]

Due to the absorption or release of latent energy, phase-change problems are nonlinear, and exact solutions are limited to a small class of problems in one-dimensional, infinite, or semi-infinite regions, with several simplifying assumptions. Numerical, finite-difference or finite-element methods offer the most practical approach for solutions to multidimensional problems. The general treatment can be conveniently divided into two groups. Single-region methods apply the energy equation once over the complete domain, covering both phases. The latent heat release is simulated by appropriate modification of the specific heat or enthalpy. Multiregion methods apply the energy equation separately for each phase and specify the proper coupling due to boundary conditions between the phases. In general, the single-region approach leads to simpler methods, whereas, the multiregion approach requires tracking the phase interface, which is an unknown function of space and time.[4] However, the one-zone models tend to be less accurate in the region near the interface since the interface is smeared over a finite region.

The heat balance integral method for solving heat transfer problems associated with solidification has been presented and its application to the continuous casting process has been illustrated by Hills and Moore.[5] Three assumptions were made in applying the integral profile technique: 1) heat conduction occurs in the transverse direction only although heat is transferred in the axial direction by the motion of the solidified material; 2) the removal of heat in the mold can be described in terms of a constant heat transfer coefficient; and 3) the liquid metal is at zero superheat throughout, and therefore, temperature gradients occur only in the solid layer. Due to the assumptions employed this method can be applied only to simplified situations. Mizikar[6] extended this integral method to solve transient, two-dimensional, heat conduction problems with solidification. Heat balances for both the solidified shell and the molten stream have been used for the analysis of the closed-mold, horizontal continuous casting system.[7] The resulting governing equations are solved by finite-difference techniques. However, these investigations ignored the axial diffusion terms, representing conduction in the withdrawal direction. Sfeir and Clumpner[8] applied the heat balance integral method to solve continuous casting of a cylindrical ingot, including the axial diffusion term in the analysis. The effect of axial conduction was found to be significant for small withdrawal speeds.

Recently, extensive analytical work on the continuous casting process has been carried out by Siegel.[9-14] Employing the conduction equations that apply in the material, the solution was obtained by using complex variable methods, particularly conformal mapping and the Cauchy integral formulation. Most of the work was directed at two-dimensional slab casting and asymmetric cases were also considered. The effects of the boundary conditions on the interface shape and the solidification rate were investigated in detail. Three-dimensional solidification was also considered. The emphasis in these articles was on the shape and characteristics of the solidification interface for an insulated mold.

Other analytical and numerical studies have been carried out on the continuous casting problem by many investigators.[15-19] The exact solution for this problem is obtained, assuming that the temperature of the incoming liquid material is uniform and equal to the solidifying temperature of the material.[15] A two-dimensional thermal model of a billet moving through the various sections of the caster is described by DeBellis and LeBeau.[16] They discussed the effects on the solidification length, shell thickness, and billet temperature profile due to changes in the process variables, such as steel grade, casting speed, and the flow rate of cooling spray. The two-region model was adopted by Kroeger and Ostrach[4] to investigate the temperature and flowfields during solidification of a pure metal in a moving slab, including natural convection or buoyancy effects in the liquid pool. A moving numerical grid and coordinate mapping procedures were used during these calculations. It was found that the buoyancy force strongly affects the flowfield but had a negligible effect on the solid-liquid interface location and shape.

Since the single-region approach (which is also called the enthalpy model or the continuum model) leads to a simpler model than the multiregion approach, this model has been employed recently to solve phase-change problems. Bennon and Incropera[20,21] used the enthalpy model to investigate the momentum, heat and species transport in binary solid-liquid phase-change problems. Hunter and Kuttler[22] solved heat conduction problems with moving boundaries associated with phase-change, combining the enthalpy method with Kirchhoff and coordinate transformations. The solidification process in the flow in a channel has also been investigated by the enthalpy method.[23] Recently, a finite-element formulation based on the enthalpy method has been developed to predict the transient field in the continuous casting process.[24] Other studies have considered continuous casting of steel employing experimental methods and various simplified models for the design of the system.[25-27] Turbulent flow in the mold region and its effect on the cast material have also been investigated.[28,29] Thus, the emphasis has been on practical processes and particular materials of interest.

In the present study a few multiregion models with the one-dimensional approximation have been analytically and numerically investigated. Simplified assumptions are made to obtain the exact solutions of the temperature distributions, the solidification thickness, and the solid-liquid interface location. The two-dimensional enthalpy method with an assumed heat transfer coefficient at the surface of the material has also been employed to solve the continuous casting problem, considering the axial diffusion term and thermal buoyancy in the liquid. The thermal field, the flowfield in the liquid zone, and the mass fraction of the liquid are obtained. The liquid-solid interface zone—in which the solid and liquid coexist—are determined by the distribution of the mass fraction of the liquid. Constant heat transfer coefficients are assumed along the mold wall and along the secondary cooling zone. The various analytical and numerical approaches are compared to indicate their limitations. The methods can be employed for many diverse manufacturing processes and the study brings out the important considerations in the modeling and simulation of such processes.

One-Dimensional Models

The difficulties in solving heat conduction problems involving phase-change arise from the nonlinear partial differential equations, which govern the problem. In general, these cannot be solved analytically and solutions must be obtained either by simplifying the physics of the problem or by using some approximate mathematical technique. In simplifying the physics of the problem, some assumptions are made to obtain analytical solutions for the continuous casting process.

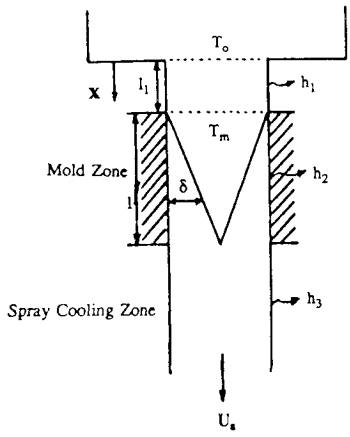

Fig. 1 Schematic diagram of the one-dimensional, three-zone model for the continuous casting process.

Three-Zone Model I

Consider molten material with uniform temperature T_0, which is higher than the solidification temperature T_m. The liquid is assumed to have cooled down to T_m when it enters the mold. The latent heat is removed in the mold zone with the temperature maintained at T_m. Therefore, solidified material at temperature T_m emerges from the mold. The cast material may be a cylindrical rod or a plate. A schematic diagram of this process is shown in Fig. 1. For a one-dimensional approximation the temperature is taken as uniform over each cross section. The thermophysical properties are taken as constant during the process. The heat transfer coefficients in the liquid, mold, and solid regions, are taken as constant at the values of h_1, h_2, and h_3, respectively. In the three-zone model I axial diffusion is neglected although this term will be included in the three-zone model II to be outlined later. The required distance from the molten liquid level to the mold inlet ℓ_1 and the mold length ℓ may be determined as the solution. The solid thickness in the mold as well as the temperature distributions along the downstream distance are also obtained.

The governing equations with the above simplified assumptions are as follows:

Liquid Region

$$\rho C U_s A \frac{dT}{dx} = -h_1 P(T - T_\infty) \tag{1}$$

Equation of the Mass Fraction of the Solid for the Mold Region

$$\rho C U_s A L \frac{dm}{dx} = h_2 P(T_m - T_\infty) \tag{2}$$

Solid Region

$$\rho C U_s A \frac{dT}{dx} = -h_3 P(T - T_\infty) \tag{3}$$

Also, the boundary conditions are

$$\begin{gathered} T(0) = T_0, \quad T(\ell_1) = T_m, \quad T(\infty) = T_\infty \\ m(\ell_1) = 0, \quad m(\ell_2) = 1.0 \end{gathered} \tag{4}$$

Equations (1–4) and the corresponding solutions are generalized by the following nondimensionalization:

$$\begin{gathered} \theta = \frac{T - T_\infty}{T_m - T_\infty}, \quad \theta_0 = \frac{T_0 - T_\infty}{T_m - T_\infty}, \quad X = \frac{x}{d}, \quad \delta^* = \frac{\delta}{d} \\ \ell^* = \frac{\ell}{d}, \quad Pe = \frac{U_s d}{\alpha_s}, \quad Bi = \frac{hd}{k_s}, \quad Ste = \frac{C(T_m - T_\infty)}{L} \end{gathered} \tag{5}$$

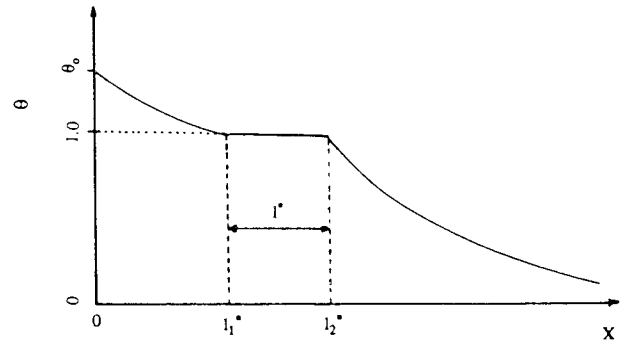

Fig. 2 Temperature profiles from the three-zone model I.

Clearly, this is a fairly idealized situation. But an analytical solution can be obtained which may be used for the validation of more accurate models.

If a cylindrical rod is produced by the continuous casting process, the ratio of A to P becomes $d/2$. The analytical solutions obtained for this case are as follows:

Liquid Region

$$\theta = \theta_0 \exp[-(2Bi_1/Pe)X] \tag{6}$$

Mold Region

$$\theta = 1.0, \quad \delta^*(X) = m(X) = (2Bi_2 Ste/Pe)(X - \ell_1^*) \tag{7}$$

Solid Region

$$\theta = \exp[-(2Bi_3/Pe)(X - \ell_2^*)] \tag{8}$$

The length ℓ_1^* from the level of the molten material to the mold inlet and the mold length, $\ell^* = \ell_2^* - \ell_1^*$, are

$$\ell_1^* = \frac{Pe}{Bi_1} \ln \theta_0, \quad \ell^* = \frac{Pe}{2Bi_2 Ste} \tag{9}$$

The resulting temperature profile is shown in Fig. 2. The distance ℓ_1^* and the mold length ℓ^* are varied, depending on the governing parameters, as given in equation (9). Similarly, solutions for other geometrics may be obtained. This model will be applicable to circumstances with small Biot numbers, so that the variations across the cast material are small. Also, axial diffusion is taken as negligible compared to the convection due to material motion. This is often valid at typical withdrawal speeds. But if U_s is small (as indicated by the Peclet number) axial diffusion effects must be included as given below.

Three-Zone Model II

The distance to the top of the mold ℓ_1 is given as an input and the axial diffusion term is considered in this model. The governing equations are as follows:

Liquid Region

$$\rho C U_s A \frac{dT}{dx} = kA \frac{d^2T}{dx^2} - h_1 P(T - T_\infty) \tag{10}$$

Equation of the Mass Fraction of the Solid for the Mold Region

$$\rho U_s A L \frac{dm}{dx} = h_2 P(T_m - T_\infty) \tag{11}$$

Solid Region

$$\rho C U_s A \frac{dT}{dx} = kA \frac{d^2T}{dx^2} - h_3 P(T - T_\infty) \tag{12}$$

The dimensionless equations are obtained, with the dimensionless variables given in Eq. (5) as follows:

Liquid Region

$$\frac{d^2\theta}{dX^2} - Pe\frac{d\theta}{dX} - 2Bi_1\theta = 0 \tag{13}$$

Solid Region

$$\frac{d^2\theta}{dX^2} - Pe\frac{d\theta}{dX} - 2Bi_3\theta = 0 \tag{14}$$

The boundary conditions with these dimensionless variables are as follows:

Liquid Region

$$\theta(0) = \theta_0 \quad \text{and} \quad \theta(\ell_1^*) = 1.0 \tag{15}$$

Solid Region

$$\theta(\ell_2^*) = 1.0 \quad \text{and} \quad \theta(\infty) = 0.0 \tag{16}$$

For the mold region, the governing equations and the boundary conditions are the same as those for the three-zone model I. Thus, the solutions for m and δ^* become identical to those given by Eq. (7). The analytical solutions for the temperature are:

Liquid Region (i.e., $0 \le X \le \ell_1^*$)

$$\theta = \{1/(e^{\lambda_1 l_1^*} - e^{\lambda_2 l_1^*})\}[(1 - \theta_0 e^{\lambda_2 l_1^*})e^{\lambda_1 X} + (\theta_0 e^{\lambda_1 l_1^*} - 1)e^{\lambda_2 X}] \tag{17}$$

Solid Region (i.e., $X \ge \ell_2^*$)

$$\theta = \exp[\lambda_3(X - \ell_2^*)] \tag{18}$$

where λ_1, λ_2, and λ_3 are as follows:

$$\lambda_1 = [(Pe + \sqrt{Pe^2 + 8Bi_1})/2]$$
$$\lambda_2 = [(Pe - \sqrt{Pe^2 + 8Bi_1})/2] \tag{19}$$
$$\lambda_3 = [(Pe - \sqrt{Pe^2 + 8Bi_3})/2]$$

The resulting temperature profiles are shown in Fig. 3. Pe is varied at fixed Bi_1 and Bi_3 in Fig. 3a, and Bi_1 or Bi_3 is varied at fixed Pe in Fig. 3b. An increase in Pe increases the convection effects (compared to axial diffusion) and the temperature delay downstream becomes more gradual due to the larger speed of material withdrawal. An increase in Biot numbers increases the cooling rates, and therefore, accelerates the temperature delay. Thus, this model is an improvement over the previous one and will apply as long as the Biot numbers are small enough to cause small variations across the cast material.

Two-Zone Model

The one-dimensional, two-zone model is applied here to investigate the continuous casting process. The axial diffusion term is again considered in this model. The schematic of the one-dimensional, two-zone model, and the relevant boundary conditions are shown in Fig. 4. The location of the liquid-solid interface is obtained as a solution. The latent heat of fusion is assumed to be released locally at the interface. The governing equations are

$$\rho C U_s A\frac{dT}{dx} = kA\frac{d^2T}{dx^2} - h_i P(T - T_\infty)$$
$$-k\left.\frac{dT}{dx}\right|_s = -k\left.\frac{dT}{dx}\right|_\ell + \rho U_s L \quad \text{at interface} \tag{20}$$

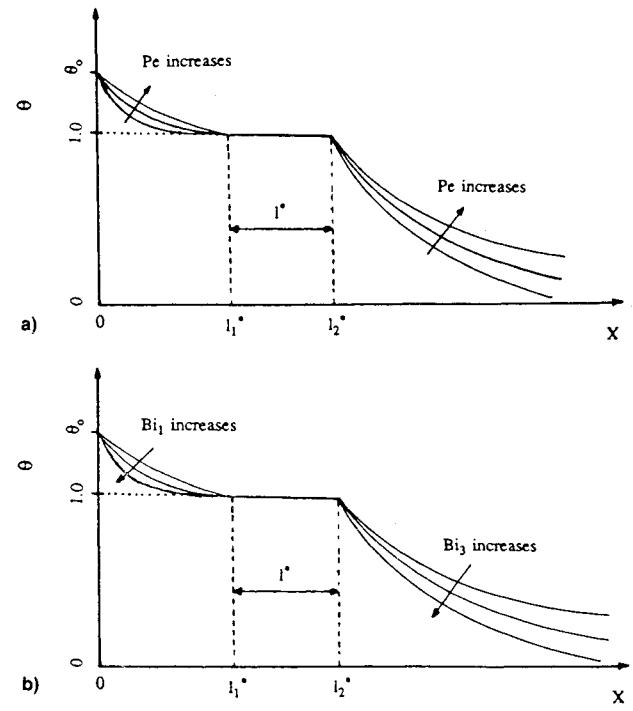

Fig. 3 Temperature profiles from the three-zone model II at a) given Biot numbers, and b) given Peclet number.

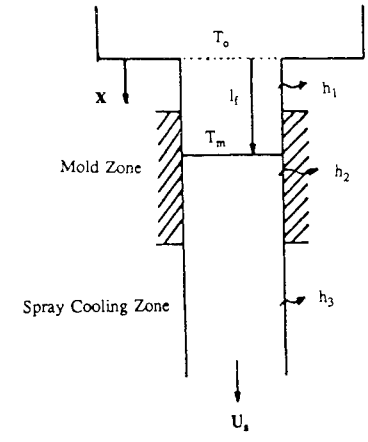

Fig. 4 Schematic diagram of the one-dimensional, two-zone model and the corresponding boundary conditions.

The dimensionless governing equations are obtained with the nondimensionalization given in Eq. (5), as

$$\frac{d^2\theta}{dX^2} - Pe\frac{d\theta}{dX} - 2Bi_i\theta = 0$$
$$-\left.\frac{d\theta}{dX}\right|_s = -\left.\frac{d\theta}{dX}\right|_\ell + \frac{Pe}{Ste} \quad \text{at interface} \tag{21}$$

The boundary conditions are as follows:

Liquid Region

$$\theta = \theta_0 \quad \text{at} \quad X = 0$$
$$\left.\frac{d\theta}{dX}\right|_\ell = \left.\frac{d\theta}{dX}\right|_s + \frac{Pe}{Ste} \quad \text{at} \quad X = \ell_f^* \tag{22}$$
$$\theta = 1.0 \quad \text{at} \quad X = \ell_f^*$$

Solid Region

$$\theta = 1.0 \quad \text{at} \quad X = \ell_f^*$$

$$\left.\frac{d\theta}{dX}\right|_s = \left.\frac{d\theta}{dX}\right|_l - \frac{Pe}{Ste} \quad \text{at} \quad X = \ell_f^* \tag{23}$$

$$\theta = 0.0 \quad \text{or} \quad \frac{d\theta}{dX} = 0, \quad \text{as} \quad X \to \infty$$

Here, ℓ_f^* is the dimensionless distance from the liquid level to the interface location. Bi_i represents the local Biot number.

The finite-difference equation is obtained by applying the three-point central difference scheme to Eq. (21). The successive over relaxation (SOR) iterative method[30] is employed. The temperature at the $(n + 1)$ iteration step is given by

$$\theta_i^{(n+1)} = \frac{\bar{\omega}}{\{Bi_i + [2/(\Delta X)^2]\}} \left\{ \left[\frac{1}{(\Delta X)^2} - \frac{Pe}{2(\Delta X)} \right] \theta_{i+1}^{(n)} + \left[\frac{1}{(\Delta X)^2} + \frac{Pe}{2(\Delta X)} \right] \theta_{i-1}^{(n+1)} \right\} + (1 - \bar{\omega})\theta_i^{(n)} \tag{24}$$

where the superscript n denotes the iteration level and $\bar{\omega}$ is the relaxation factor, with $1 < \bar{\omega} < 2$.

The iterative method starts with a guessed initial field and sequentially improves the field by using successive iterations until convergence is achieved. The solid-liquid interface location ℓ_f^* is changed within the tolerance which is taken here as $\Delta X = 0.05$. When the solidification temperature $\theta = 1.0$ is located between the grid points the interface location ℓ_f^* is calculated by interpolation.

The numerical results for the boundary conditions $\theta = 0$ and $d\theta/dX = 0$ far downstream—taken as $X = 100$ here—are obtained and found to be identical. This implies that any kind of downstream boundary condition (Dirichlet or Neumann) is satisfactory for this problem if the condition is specified far enough downstream. The location of the downstream boundary location was also varied from $X = 20$ to $X = 100$, and it was found that $X = 20$ is large enough when the Neumann boundary condition is applied there. A larger value was found to be satisfactory for the Dirichlet condition.

The numerical solutions with the Neumann boundary condition at $X = 20$ were obtained for different values of the governing parameter *Ste*. The calculated temperature distributions are shown for various *Ste* in Fig. 5 at $Pe = 1.0$, $Bi_1 = 0.0$, $Bi_2 = 0.1$, and $Bi_3 = 0.5$. The mold is located in the region from $X = 4$ to $X = 10$. The solid-liquid interface location is easily found by tracking the dimensionless temperature $\theta = 1.0$ or the discontinuity in the temperature gradient, which is imposed by the boundary condition at the interface.

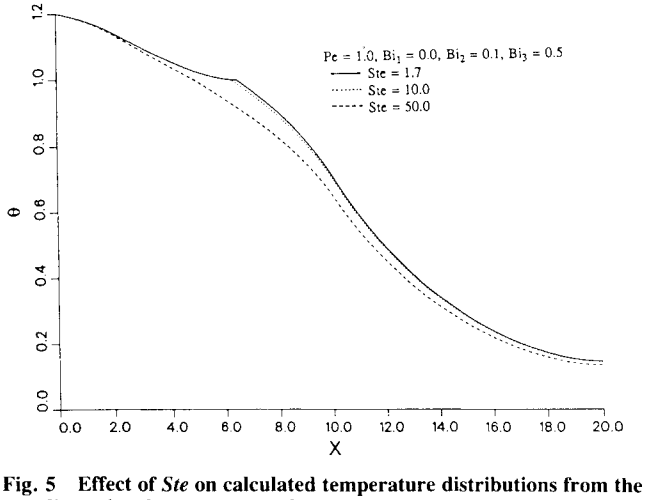

Fig. 5 Effect of *Ste* on calculated temperature distributions from the one-dimensional, two-zone model.

As seen in this figure the interface location moves upstream as *Ste* increases. However, the results are not affected significantly by changing *Ste* from 1.7 to 10.0. According to the nondimensionalization at very large values of *Ste*, the problem approaches the single-phase problem since L approaches zero. With $Ste = 50$ the interface location is hard to pick from the discontinuity of the temperature gradient. This implies that the case of $Ste = 50$ is very close to the conduction problem with no phase change. This model, therefore, allows a computation of the interface location as well as the temperature field. Variations across the material are neglected, as done for earlier models. But the interface location is determined as a function of the operating conditions. This model will be particularly useful for cases that involve a fairly flat interface such as that for insulated molds.[9, 12] Again, the model is an idealized one and can be used for the validation of two- and three-dimensional models that may be employed for more complicated situations.

Two-Dimensional Enthalpy Model

Analysis

Consider the molten material fed at $x = 0$ with laminar flow at a uniform feed velocity U_s over the entire cross section and with constant temperature $T_0 > T_m$. The temperature and flowfields in the liquid, the temperature distribution in the solid, the effect of thermal buoyancy, and the interface position and shape during steady-state operation are of particular interest in the process. The steady-state process is governed by the conservation equations for mass, momentum, and energy, which may be expressed in continuum form as[31]

$$\nabla \cdot (\rho \vec{v}) = 0$$

$$\frac{\partial \vec{v}}{\partial t} + \vec{v} \cdot \nabla \vec{v} = -\frac{\nabla p}{\rho} + \nabla \cdot (\nu \nabla \vec{v}) + \bar{g}\beta(T - T_s) \tag{25}$$

$$\rho \frac{\partial H}{\partial t} + \rho \vec{v} \cdot \nabla H = \nabla \cdot (k \nabla T)$$

Each of the phase enthalpies is defined as

$$H_k = \int_0^T C_k \, dT + H_k^0 \tag{26}$$

Thus, the phase enthalpies defined by Eq. (26) are related to the temperature by the expressions

$$H_s = C_s T; \qquad H_l = C_l T + [(C_s - C_l)T_m + L] \tag{27}$$

Except for obtaining the buoyancy force term in the momentum equation, the continuum density ρ is assumed to be constant, i.e., the Boussinesq approximations are employed.[30,31] The continuum enthalpy and thermal conductivity are defined as

$$H = H_s + f_l(H_l - H_s); \qquad k = k_s + f_l(k_l - k_s) \tag{28}$$

Here f_l is expressed from equilibrium thermodynamic considerations as

$$f_l = \begin{cases} 0 & H \le C_s T_m \\ (H - C_s T_m)/L & C_s T_m < H < (C_s T_m + L) \\ 1 & (C_s T_m + L) \le H \end{cases} \tag{29}$$

The thermophysical properties of each phase are also assumed constant, and the continuum dynamic viscosity ν is expressed as the harmonic mean of the phase viscosities in

the limit $\nu_s \to \infty$. Therefore

$$\nu = (\nu_l/f_l) \tag{30}$$

The assumption of constant values of the specific heats and the thermal conductivities of each phase is a computational simplification suitable for solidification occurring over moderate temperature ranges.

The pressure term in Eq. (25) is eliminated by taking the curl of the momentum equation and transforming it into the vorticity transport equation, as outlined by Jaluria and Torrance.[30] ψ and ω are defined as

$$u = \frac{\partial \psi}{\partial y}, \quad v = -\frac{\partial \psi}{\partial x}, \quad \omega = \frac{\partial v}{\partial x} - \frac{\partial u}{\partial y} \tag{31}$$

Equations (25) and (31) are nondimensionalized by employing the following transformations:

$$X = \frac{x}{d}, \quad Y = \frac{y}{d}, \quad \tau = \frac{tU_s}{d}, \quad U = \frac{u}{U_s}, \quad V = \frac{v}{U_s}$$

$$\Psi = \frac{\psi}{U_s d}, \quad \Omega = \frac{\omega d}{U_s}, \quad \theta = \frac{T - T_s}{T_m - T_s}$$

$$H^* = \frac{H}{L}, \quad k_r = \frac{k}{k_s}, \quad \nu_r = \frac{\nu}{\nu_l}, \quad Bi = \frac{hd}{k}, \quad Re = \frac{U_s d}{\nu_l}$$

$$Pe = \frac{U_s d}{\alpha_s}, \quad Gr = \frac{g\beta(T_0 - T_m)d^3}{\nu_l^2}, \quad Ste = \frac{C_s(T_m - T_s)}{L} \tag{32}$$

The dimensionless equations thus obtained in the vorticity-stream function formulation become

$$\nabla^{*2}\Psi = -\Omega$$

$$\frac{\partial \Omega}{\partial \tau} + \bar{V}\cdot\nabla^*\Omega = \frac{1}{Re}[\nabla^*\cdot(\nu_r\nabla^*\Omega)] + \frac{Gr}{Re^2}\frac{\partial \theta}{\partial Y} \tag{33}$$

$$\frac{\partial H^*}{\partial \tau} + \bar{V}\cdot\nabla^* H^* = \frac{Ste}{Pe}[\nabla^*\cdot(k_r\nabla^*\theta)]$$

It is noted that Pe in the energy equation is dependent upon only the properties of the solid and not on the properties of the liquid since the dimensionless quantity k_r is based on the solid thermal conductivity k_s.

The boundary conditions on u, v, and T are obtained from the physical considerations of the continuous casting process. Generally, these are the uniform temperature T_0, higher than the fusion temperature T_m of the molten material at the inlet, and the constant withdrawal speed U_s of the solidified material at the outlet. Additional boundary conditions downstream—in X—are needed for temperature because of the elliptic nature of the governing equations. The developed conditions on the temperature field far downstream are applied here, as discussed for the one-dimensional, two-zone model. The boundary conditions in terms of Ω and Ψ were obtained by employing the appropriate transformation of the physical boundary conditions.[30]

Numerical Scheme

Numerical calculations were carried out only for half of the physical domain of the process because of symmetry in two-dimensional, planar, continuous casting. Since each of the continuum Eqs. (33) is valid throughout the entire solution domain, the need for moving numerical grids, coordinate mapping, and boundary conditions at the phase interface between solid and liquid is eliminated. Thus, only the externally imposed boundary conditions are needed—as with conventional single-phase analysis.

The full equations are solved by finite-difference methods, employing the ADI scheme.[30] A uniform grid in the computational domain and the central difference scheme for the advection and diffusion terms are used. The sequence of the numerical operations is identical to that used to solve conventional single-phase problems. Since the vorticity and energy equations are coupled, an iterative procedure is adopted. Within this iterative scheme, Eqs. (27–30) provide the necessary descriptions of the temperature fields for the evaluation of the buoyancy term, as well as the liquid mass fraction distributions for the evaluation of continuum dynamic viscosity and thermal conductivity. The numerical scheme was validated by considering heated moving fluid in channels, without phase change. Also, the grid was refined and the results obtained were found to be independent of further refinement. Several similar heat transfer and flow problems were considered to ensure that the numerical scheme was accurate and consistent. These results are not discussed here for conciseness. However, the scheme is versatile and can be used for a variety of moving materials undergoing thermal processing.

Numerical Results and Discussions

The numerical scheme (based on the enthalpy method) has been employed to investigate a continuous casting process. The scheme, developed in the present study, has been applied to an insulated mold[11] and the results obtained by the present enthalpy method are compared with the analytical solutions by Siegel.[11] A schematic diagram of the insulated mold is shown in Fig. 6. The geometry and boundary conditions are also given in this figure. The x coordinate starts at the top of the insulated mold in the downstream direction and y indicates the distance from the mold in the transverse direction. Since the characteristic length is the half-thickness of the planar mold, $Y = 0$ is the mold wall and $Y = 1.0$ is the centerline of the moving material. A superheated liquid at a uniform temperature $T_0 > T_m$ enters the insulated mold at a uniform feed velocity U_s. To remove heat from the moving material the ingot below the mold is assumed to be cooled by an efficient convective heat transfer mechanism so that the sides are at T_s. It is noted here that the Re and Gr are not independent variables since these parameters are incorporated in Pe and inlet temperature θ_0 of the liquid material. If a material is chosen and the inlet temperature T_0 of the liquid material

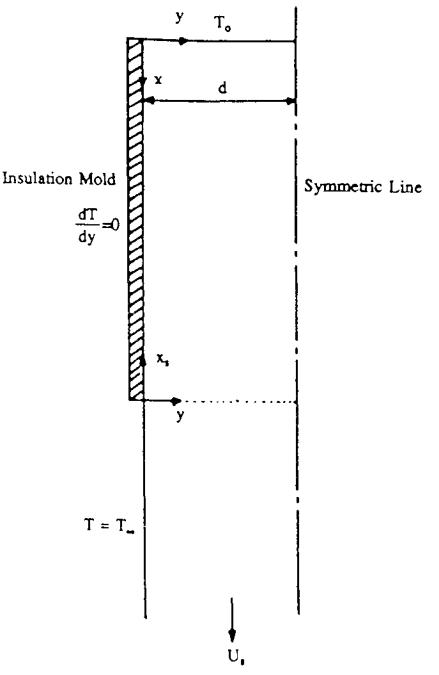

Fig. 6 Schematic diagram of an insulated mold.

is specified, *Ste* and *Gr* are automatically determined. The Reynolds number is related to the Peclet number. Thus, the governing parameters are selected as *Ste*, *Pe*, θ_0, and the cooling rate *Bi*.

A comparison is made between the liquid-solid interface zone obtained by the enthalpy method and the analytical solution of Siegel[11] in Fig. 7. In this figure, the shaded area indicates the liquid-solid interface region and the upper and lower lines of the shaded area the boundaries of this region. Another coordinate x_s, which starts from the bottom of the insulated mold in the upstream direction, is employed to make the comparison easier. Here, the length of the insulated mold is taken as $3d$. It was assumed by Siegel that the cast material is withdrawn very slowly so that the convection transport may be ignored relative to conduction transport for simplification in the calculations. He also assumed that the latent heat of fusion is removed locally along the interface, an assumption usually employed in two-zone models. A discontinuity exists in the temperature gradient at the interface location. Thus, the analytical solution of the interface is represented by a line, not an area as obtained by the enthalpy method. A good agreement between the two results is found when the value of *Pe*/*Ste* is small. However, a large deviation is seen in this figure when *Pe*/*Ste* is 1.0. This implies that the simplifying assumption in Siegel's model (i.e., very slow withdrawal rate of the cast material and negligible convection), fails with an increase in the withdrawal speed U_s, as expected. Also, an increase in *Pe*/*Ste* results in the interface moving downward, as expected for increasing withdrawal speed. The curvature of the interface is also larger for interfaces that are at a lower position, implying larger temperature variation across the cast material. The temperature field depends on the inlet temperature, material, withdrawal speed, etc., and a significant variation with *y* arises in several cases, as seen here.

In order to apply the enthalpy method, another situation of the continuous casting process is considered. It is assumed that a constant heat transfer coefficient exists at the mold and heat is also extracted in the spray cooling zone. This is usually the case in typical continuous casting processes.[2] In the mold the molten material is cooled indirectly, e.g., by circulating cooling water through the jacket adjacent to the mold walls. However, the solidified material beyond the mold can be cooled directly, e.g., by water spray cooling. Therefore, thermal energy is extracted at a faster rate in the spray cooling zone than in the mold. A schematic of the process and the relevant boundary conditions for this circumstance are shown in Fig. 8. The aspect ratio is taken as 20. This aspect ratio was found to be adequate to satisfy the boundary condition of a developed temperature distribution at $X = 20$. Mold cooling is assumed to apply from $X = 2.0$ to $X = 10.0$, and secondary cooling from $X = 10.0$ to $X = 20.0$ in this case.

Isotherms and the shape of the liquid-solid interface zone obtained numerically are shown in Figs. 9 and 10 for various conditions. It was found that the streamlines are straight and the flow is very uniform. Thus, for the conditions considered here, buoyancy effects are small. At larger temperature differences, the effects were found to be larger, as expected.[32] The enthalpy model yields a region over which the phase

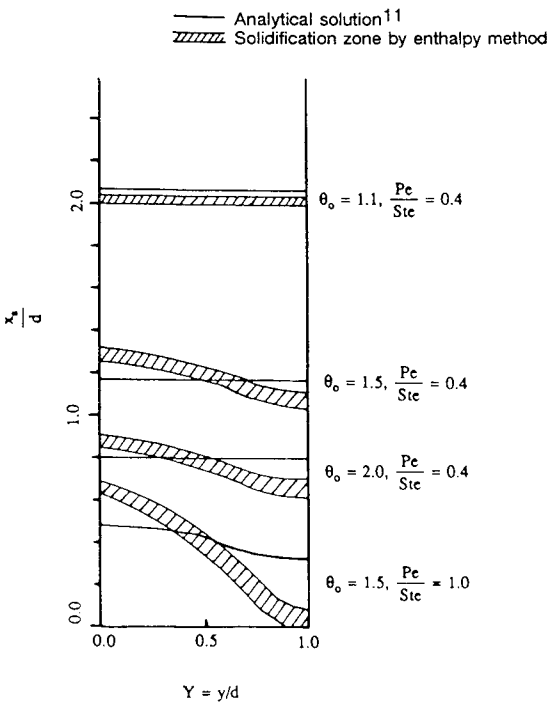

Fig. 7 Comparison between the present results and the analytical solution for the interface from Siegel.[11]

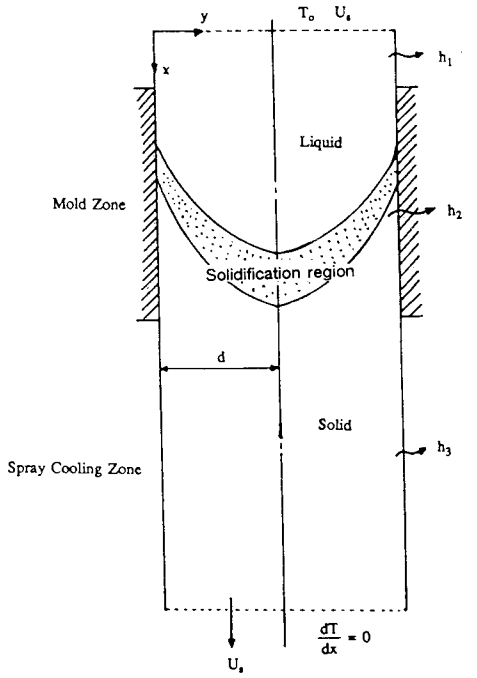

Fig. 8 Schematic diagram of a continuous casting process for a constant heat transfer coefficient at the mold and spray cooling downstream, with the boundary conditions.

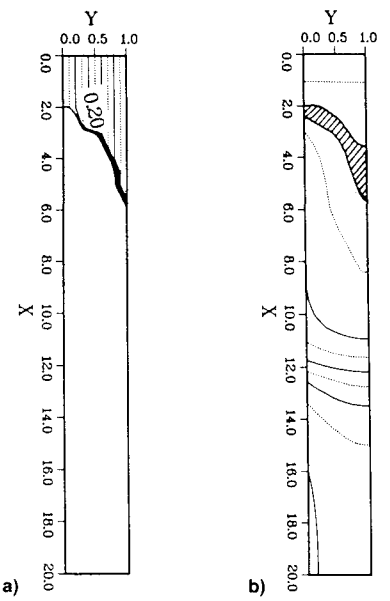

Fig. 9 Computed streamlines and isotherms for aluminum at *Ste* = 2.5, *Pe* = 0.8, $Bi_1 = 0.0$, $Bi_2 = 0.1$, and $Bi_3 = 0.5$: a) streamlines, and b) isotherms.

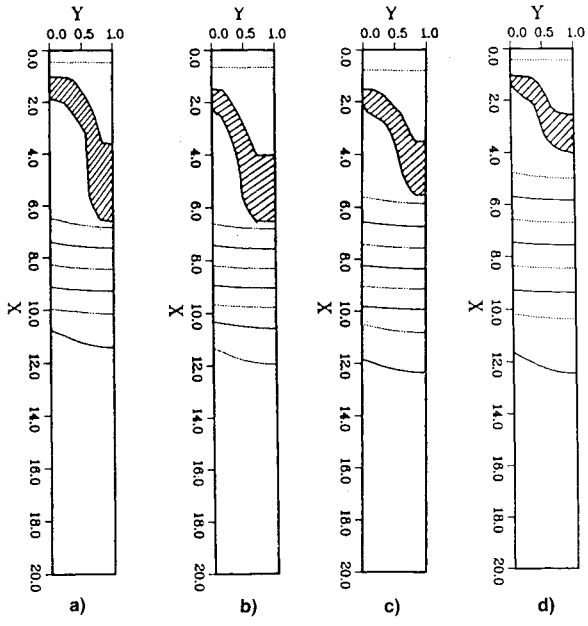

Fig. 10 Computed isotherms for various Pe at $\theta_0 = 1.2$, $Bi_1 = 0.0$, $Bi_2 = 0.1$, and $Bi_3 = 0.5$, showing the effect of material on the results from the enthalpy method: a) $Pe = 1.0$, $Ste = 2.65$ for n-octadecane; b) $Pe = 0.5$, $Ste = 2.65$ for n-octadecane; c) $Pe = 0.3$, $Ste = 2.65$ for n-octadecane; and d) $Pe = 0.3$, $Ste = 2.5$ for aluminum.

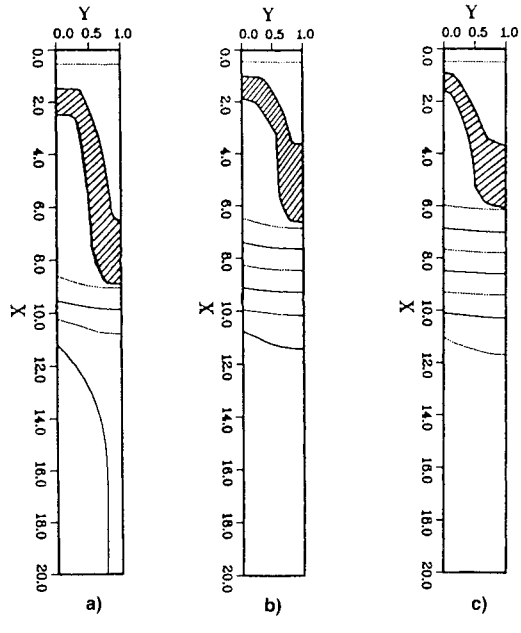

Fig. 11 Effect of the cooling rate at the mold Bi_2 on the results by the enthalpy method for n-octadecane at $Ste = 2.65$, $Pe = 1.0$, $Bi_1 = 0.0$ and $Bi_3 = 0.5$: a) $Bi_2 = 0.05$, b) $Bi_2 = 0.1$, and c) $Bi_2 = 0.15$.

change occurs. Due to heat removal from the molten material at the mold sides, a solid skin is formed, retaining some liquid in the core of the mold. Thus, depending on the governing parameters, the shape of the interface zone may not be flat. The effects of the withdrawal speed U_s on the isotherms and on the shape of the solidification region are shown in Fig. 10 for n-octadecane at $Ste = 2.65$, $\theta_0 = 1.2$, $Bi_1 = 0.0$, $Bi_2 = 0.1$, and $Bi_3 = 0.5$. As expected, the liquid-solid interface zone moves downstream as Pe is increased. The properties of aluminum are applied to the enthalpy method to see the effect of a different material. When a different material is used, Ste changes and the thermal properties, such as ν_s and k_s, are also affected. The results for aluminum at $Ste = 2.5$, $Pe = 0.3$, $\theta_0 = 1.2$, $Bi_1 = 0.0$, $Bi_2 = 0.1$, and $Bi_3 = 0.5$ are shown in Fig. 10d. It is found that the upstream conduction

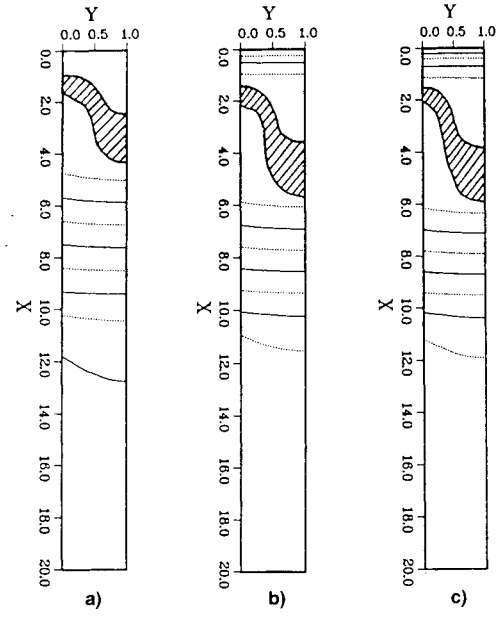

Fig. 12 Effect of the liquid inlet temperature θ_0 on the isotherms for n-octadecane at $Ste = 2.65$, $Pe = 1.0$, $Bi_1 = 0.0$, $Bi_2 = 0.1$, $Bi_3 = 0.5$: a) $\theta_0 = 1.1$, b) $\theta_0 = 1.4$, and c) $\theta_0 = 1.5$.

effect is very significant for aluminum due to the high thermal conductivity of the material. Thus, the solidification process for aluminum starts earlier and finishes earlier than that for n-octadecane.

The effect of the cooling rate at the mold as given by Bi_2, is also shown in Fig. 11 for n-octadecane. The trends are very similar to those from the one-dimensional, two-zone model. It is found that the solidification process starts farther upstream as the cooling rate is increased. As expected, the solidification region moves downstream as cooling rate is decreased. The cooling rate also affects the temperature distribution downstream of the solidification region. The effect of Gr on the results is studied by varying the liquid inlet temperature θ_0. Figure 12 shows the results when θ_0 is varied from 1.1 to 1.5 for n-octadecane. It is seen that, as expected, the solidification region moves downstream with increasing θ_0 and the temperature variation across the cast material also increases. The streamlines were not found to be significantly affected by this variation in θ_0. For brevity, only a few typical results are shown here. The main thrust of the study was to demonstrate the use of the enthalpy method for this problem and to evaluate axial conduction and buoyancy effects, solving the full elliptic equations. The approach can be used for a wide range of materials and operating conditions, with or without phase change.[32]

These results are valuable in the evaluation of the effects of the various physical variables in the problem such as cooling rate at the mold and withdrawal speed of the cast material, etc., on the position and shape of the interface zone. Since a flat interface is desirable to get better uniformity in the cast product, the interface shape may be controlled by varying the cooling rate in the mold or the withdrawal speed of the cast material. However, the productivity is decreased by reducing the withdrawal speed, and the production cost is increased by increasing the cooling rate. Several other circumstances were considered and similar trends were obtained. The results presented here are of interest and importance in obtaining a better control of existing continuous casting processes leading to improved product quality and increased productivity, and for the design and optimization of future systems.

Conclusions

Two simple one-dimensional, three-zone models are developed for continuous casting and other phase-change processes,

and are solved analytically. A one-dimensional, two-zone model for the continuous casting process is also developed and solved numerically, employing the finite-difference method. Simplifications are made to obtain exact solutions of the temperature distributions, the solidified material thickness, and the solid-liquid interface location. The results are found to follow the expected physical trends and to agree with results in the literature. A two-dimensional enthalpy model has also been developed to solve the continuous casting problem, considering axial diffusion and thermal buoyancy effects. The thermal field, flowfield in the liquid zone, and the mass fraction of the liquid are calculated.

The results obtained show good agreement with earlier analytical solutions when the Peclet number is small (which was assumed to be the case in the earlier analytical model). As the Peclet number is increased, a solid skin is formed at the sides of the mold wall while liquid still exists in the core region. The shape of the interface can be controlled by varying the governing parameters for better product quality. It is also found that, as expected, the liquid-solid interface position moves downstream as Pe or θ_0 increases or as the cooling rates are decreased. This article presents a few analytical and numerical approaches to the simulation of a continuously moving material undergoing a phase-change process. These are applied to continuous casting and the results obtained are compared with those in the literature. However, the methods can be employed for other phase-change processes in moving materials, such as crystal growing, plastic extrusion, and glass fiber drawing.

Acknowledgment

The authors acknowledge the financial support for this work provided by the National Science Foundation under Grants CBT-88-03049 and INT-88-13510.

References

[1]Kalpakjian, S., *Manufacturing Processes for Engineering Materials*, Addison-Wesley, Reading, MA, 1985, pp. 257–258.

[2]Pollack, H. W., *Materials Science and Metallurgy*, 4th ed., Prentice Hall, Englewood Cliffs, NJ, 1988, pp. 28–30.

[3]Doyle, L. E., *Manufacturing Processes and Materials for Engineering*, 3rd ed., Prentice Hall, Englewood Cliffs, NJ, 1989, pp. 193–195.

[4]Kroeger, P. G., and Ostrach, S., "The Solution of a Two-Dimensional Freezing Problem Including Convection Effects in the Liquid Region," *International Journal of Heat Mass Transfer*, Vol. 17, No. 10, 1974, pp. 1191–1207.

[5]Hills, A. W. D., and Moore, M. R., "Use of Integral-Profile Methods to Treat Heat Transfer During Solidification," edited by A. W. D. Hills, *Heat and Mass Transfer in Process Metallurgy*, Inst. of Mining and Metallurgy, 1967, pp. 141–171.

[6]Mizikar, E. A., "Mathematical Heat Transfer Model for Solidification of Continuously Cast Steel Slabs," *Transactions of the Metallurgical Society of AIME*, Vol. 239, 1967, pp. 1747–1753.

[7]Stanek, V., and Szekely, J., "A Mathematical Model of the Closed Mold (Watts) Horizontal Continuous Casting Process," *Metallurgical Transactions B*, Vol. 7B, 1976, pp. 619–630.

[8]Sfeir, A. A., and Clumpner, J. A., "Continuous Casting of Cylindrical Ingots," *Journal of Heat Transfer*, Vol. 99, No. 1, 1977, pp. 29–34.

[9]Siegel, R., "Shape of Two-Dimensional Solidification Interface During Directional Solidification by Continuous Casting," *Journal of Heat Transfer*, Vol. 100, No. 1, 1978, pp. 3–10.

[10]Siegel, R., "Analysis of Solidification Interface Shape During Continuous Casting of a Slab," *International Journal of Heat Mass Transfer*, Vol. 21, No. 11, 1978, pp. 1421–1429.

[11]Siegel, R., "Two-Region Analysis of Interface Shape in Continuous Casting with Superheated Liquid," *Journal of Heat Transfer*, Vol. 106, No. 3, 1984, pp. 506–511.

[12]Siegel, R., "Control of Solidification Boundary in Continuous Casting by Asymmetric Cooling and Mold Offset," *International Journal of Heat Mass Transfer*, Vol. 28, No. 2, 1985, pp. 500–502.

[13]Siegel, R., "Analysis of Three-Dimensional Solidification Interface Shape," *International Journal of Heat Mass Transfer*, Vol. 28, No. 3, 1985, pp. 701–705.

[14]Siegel, R., "Free Boundary Shape of a Convectively Cooled Solidified Region," *International Journal of Heat Mass Transfer*, Vol. 29, No. 2, 1986, pp. 309–315.

[15]Blackwell, J. H., and Ockendon, J. R., "Exact Solution of a Stefan Problem Relevant to Continuous Casting," *International Journal of Heat Mass Transfer*, Vol. 25, No. 7, 1982, pp. 1059–1060.

[16]DeBellis, C. L., and LeBeau, S. E., "A Verified Thermal Model for Continuous Casting Processes," edited by R. K. Shah, *Heat Transfer in Manufacturing and Materials Processing, ASME 1989 National Heat Transfer Conference*, NY, 1989, pp. 105–111.

[17]Sen, A. K., "Perturbation Solutions for the Shape of a Solidification Interface Subjected to Spatially Periodic Heat Flux," *Journal of Heat Transfer*, Vol. 109, No. 4, 1987, pp. 835–840.

[18]Yao, L. S., "Natural Convection Effects in the Continuous Casting of a Horizontal Cylinder," *International Journal of Heat Mass Transfer*, Vol. 27, No. 5, 1984, pp. 697–704.

[19]Szekely, J., Evans, J. W., and Brimacombe, J. K., "Modeling of the Continuous Casting of Steel," *The Mathematical and Physical Modeling of Primary Metals Processing Operations*, Wiley-Interscience, New York, 1988, Chap. 7, pp. 197–227.

[20]Bennon, W. D., and Incropera, F. P., "A Continuum Model for Momentum, Heat and Species Transport in Binary Solid-Liquid Phase Change Systems—I. Model Formulation," *International Journal of Heat Mass Transfer*, Vol. 30, No. 10, 1987, pp. 2161–2170.

[21]Bennon, W. D., and Incropera, F. P., "A Continuum Model for Momentum, Heat and Species Transport in Binary Solid-Liquid Phase Change Systems—II. Application to Solidification in a Rectangular Cavity," *International Journal of Heat Mass Transfer*, Vol. 30, No. 10, 1987, pp. 2171–2187.

[22]Hunter, L. W., and Kuttler, J. R., "The Enthalpy Method for Heat Conducting Problems with Moving Boundaries," *Journal of Heat Transfer*, Vol. 111, No. 2, 1989, pp. 239–242.

[23]Bennon, W. D., and Incropera, F. P., "Developing Laminar Mixed Convection with Solidification in a Vertical Channel," *Journal of Heat Transfer*, Vol. 110, No. 2, 1988, pp. 410–415.

[24]Chidiac, S. E., Samarasekera, I. V., and Brimacombe, J. K., "A Numerical Method for Analysis of Phase Change in the Continuous Casting Process," *Numiform 89*, edited by E. C. Thompson, R. D. Wood, O. C. Zienkiewicz and A. Samuelson, A. A. Balkema, The Netherlands, 1989, pp. 121–128.

[25]Brooks, M. G., "IISI Survey of Continuous Casting Technology," *Solidification Processing 1987, Proceedings of 3rd International Conference*, Univ. of Sheffield, Inst. of Metals, UK, 1987, pp. 231–234.

[26]Brimacombe, J. K., and Weinberg, F., "Continuous Casting of Steel, Part II: Theoretical and Measured Liquid Pool Profiles in the Mold Region," *J. Iron Steel Inst.*, Vol. 211, 1973, pp. 24–33.

[27]Brimacombe, J. K., Samarasekera, I. V., and Bommoraju, R., "Optimum Design and Operation of Models for Continuous Casting of Steel Billets," *Steelmaking Proc.*, Vol. 69, 1986, pp. 409–423.

[28]Asai, S., and Szekely, J., "Turbulent Flow and Its Effects in Continuous Casting," *Ironmaking and Steelmaking*, Vol. 3, 1973, pp. 205–213.

[29]Szekely, J., and Yadoya, R. T., "The Physical and Mathematical Modeling of the Flow Field in the Mold Region in Continuous Casting Systems: Part II, The Mathematical Representation of Turbulent Flow," *Metallurgical Transactions*, Vol. 4, 1973, pp. 1379–1388.

[30]Jaluria, Y., and Torrance, K. E., *Computational Heat Transfer*, Hemisphere, New York, 1986, Chap. 5.

[31]Jaluria, Y., *Natural Convection Heat and Mass Transfer*, Pergamon, Oxford, England, UK, 1980, Chap. 2.

[32]Kang, B. H., Conjugate Heat Transfer From a Continuously Moving Material and From an Isolated Heat Source," Ph.D. Dissertation, Rutgers Univ., New Brunswick, NJ, 1990.